Original Research

Microwave-Assisted Hydrothermal Carbonization of Furfural Residue for Adsorption of Cr(VI): Adsorption and Kinetic Study

Shujauddin Khushk[1], Lei Zhang[1, 2]*, Aimin Li[1], Muhammad Irfan[1], Xiaojuan Zhang[1]

[1]School of Environmental Science and Technology, Dalian University of Technology, Dalian, P. R. China
[2]State Key Laboratory of Petroleum Pollution Control, CNPC Research Institute of Safety and Environmental Technology, Beijing, China

Abstract

The existence of heavy metals on the earth's surface and disposal of industrial effluents to the environment causes severe health issues that need to be dealt with. Adsorption of Cr(VI) was carefully studied onto the furfural residue in a batch system. Furfural residue was treated in the microwave-assisted HTC with water as an effective medium, and the subsequent solid material was further treated by a low concentration of potassium hydroxide. Under optimum conditions (pH 2, 25ºC, and 2.5 g/L adsorbent dosage), 91.72% Cr(VI) was removed at the initial concentration of 100 mg/L to achieve equilibrium condition. The effects directed that a higher adsorption capacity of Cr(VI) (36.91 mg/g) was reached by integrating microwave-assisted treatment at 200ºC and 0.05 N KOH concentration. Important parameters like effect of pH, contact time, temperature and solution concentration were optimized to investigate their effectiveness. The experimental adsorption data were best fit for the Freundlich model, which instantly followed the pseudo second-order kinetics model. Investigation of thermodynamic studies demonstrated negative values. The findings of the study suggested the modified hydrochar generated from furfural residue could be considered as an alternative to high-cost adsorbents.

Keywords: adsorption, Cr(VI), furfural residue, kinetics isotherms, microwave-assisted HTC

Introduction

The growing population and increasing demand for healthy water for drinking and agriculture use have brought many challenges today. Chromium (Cr) is considered as the primary metal pollutant because it is found in large amounts in such modern industries as textiles, leather tanning, metal alloys, plastics, cement, mining, and wood. Its existence in the water causes severe diseases like lung cancer and DNA strand breaks (U.S. National Toxicology Program) [1-3]. An acceptable concentration limit of chromium in the drinking water is 0.05 mg/L (WHO) [4].

Several conventional tactics have been applied for Cr(VI) removal of dissolved metals, for instance electro-dialysis [4], membrane technology [5], reverse osmosis, chemical coagulation, ion exchange and others [6].

*e-mail: zhanglei78@dlut.edu.cn

However, these techniques have revealed limitations due to high economic rates, high-energy consumption and non-suitability to environmental conditions. Conversely, the adsorption method has gained high attention because of its suitable economic rates, high efficiency, an easily designed process and stable performance [7, 8]. For adsorption, the most important element is to prepare an adsorbent, which addresses the key aspects to eliminate a defined pollutant's removal efficiency, process and its cost management.

Commercial activated carbon is widely used as an adsorbent, but its cost management and redevelopment is challenging. Hence, several materials have been broadly studied such as animal wastes, agricultural wastes, and clays to prepare adsorbent [1]. The material which we had prepared for removal of Cr(VI) had never been used by any researcher for an adsorption process. This adsorbent can help the purification industry to remove Cr(VI) through a microwave-assisted treatment method by improving its efficiency with minimum resources.

Microwave-assisted hydrothermal carbonization has made it more modest than manual heating (or conventional) machine setup. Therefore, this technique is considered the best technology for economic stability because of its inherent advantages such as numerous end products [9]. Compared with the conventional HTC method, microwave-assisted HTC is likely the more efficient, faster, and appropriate method. This method has the potential to effective depolymerize and decrystalize cellulose during microwave-assisted reaction under low temperatures, which has been reported in studies [10]. Furthermore, Elaigwu and Greenway studied the comparison between conventional and microwave-assisted HTC of lignocellulosic waste material, where microwave-assisted HTC was shown to rapidly decompose the waste material in terms of time compared with the conventional method [11]. The temperature range for the microwave-assisted heating is suggested as being 180-250ºC at 0.5 hours [9]. Characteristically, biomass thermal degradation is a source of getting activated carbon that is a carbonaceous material, where water is used as a medium, followed by two steps of activation. In addition, high porosity and surface area of activated carbon must be considered. The greater the pore structure the higher the adsorption capacity [12].

Corncob residues, cottonseed hulls, oat hulls, and sugarcane processing are the sources of preparation for furfural residue after the bio-refinery process, where furfural residue is considered waste. These agriculture materials are waste lignocellulose substances, adding a certain volume of acid (5-8% dilute H_2SO_4) tends to hydrolysis reaction at a particular temperature (175-185ºC) and pressure. Later, the extracted chemical substance having furfural form and the remaining amount is furfural residue, which is rich in lignin and cellulose [13]. It has been calculated that about 23 million tons/year of furfural residue is generated in China only. Approximately 12 to 15 tons of furfural residues are required to prepare 1 ton of furfural chemical [14]. Almost 40% of carbon is found in furfural residue, so its approach as an adsorbent for the wastewater industry is of great importance. Unluckily, a huge amount of furfural residue stayed either unused or fired in an open atmosphere, which causes several health and environmental problems. Furfural residue possesses a great potential to be utilized for adsorption of heavy metals from wastewater. Hence, the synthesis of furfural residue was carried out using the microwave-assisted HTC process for adsorption of Cr(VI).

The key objective of this research is to introduce furfural residue as a highly efficient adsorbent (hydrochar) after its microwave-assisted HTC and alkali treatment. In addition, we demonstrated the adsorption capacity of the enhanced hydrochar towards Cr(VI) from wastewater by determining the adsorption capacity, kinetics study, adsorption isotherms, and thermodynamics. The process that we selected is very simple and low cost. We examined the effects of key parameters, for instance solution pH, contact time, temperature, concentration of chromium ions and alkali treatment for the capacity level of the hydrochar adsorption. Furthermore, the furfural residue was characterized by Fourier transform infra-red (FTIR), scanning electron microscopy (SEM), and Buraner-Emmett-Teller (BET).

Materials and Methods

Reagents

Hydrochloric acid (HCl), acetone (C_3H_6O), sulphuric acid (H_2SO_4), potassium hydroxide (KOH), potassium dichromate ($K_2Cr_2O_7$), phosphoric acid (H_3PO_4), 1-5 diphenylcarbazide ($C_{13}H_{14}N_4O$).

Preparation of Raw Material and Microwave-Assisted HTC

Furfural residue (FR) was delivered by the furfural production industry located in Dalian, China. Initially, FR was washed with distilled water to remove its soluble impurities. Secondly, it was dried at 105ºC in the oven for 24 h to eliminate volatile impurities and moisture content. Finally, it was crushed, and the particles size of 0.30-0.40 mm were collected for further experiments.

The microwave-assisted HTC method was carried out by using a sealed reactor (Nickled Alloy GFC 625 type) in the microwave-assisted machine. An amount of 2 g furfural residue and 14 mL DW (biomass-to-water ratio 1:7) was subjected to the microwave-assisted carbonization at 200ºC for 30 min with a power of 600 W. After treatment, the reactors were left for cooling to room temperature, and later the mixture was separated using a 0.45 μm filtration membrane. Furfural residue was called hydrochar. Its pH was checked and adjusted to neutral by washing the hydrochar repeatedly.

The hydrochar was confined in the appliance at 105ºC for overnight and then saved in a sealed tube for further analysis [15].

Modification of Prepared Hydrochar

Prepared hydrochar was treated with low concentrations of KOH (or HCl). Three concentrations of KOH (or HCl) and hydrochar were mixed in a magnetic stirrer having solution ratio of 1:50 (w/v) for 60 min at 30°C. The mixture was separated by a 0.45 µm membrane after transferring into a Buchner funnel. The pH of the filtered residue was adjusted to neutral by washing the filtrate with distilled water. Finally, hydrochar was confined in the appliance at 105ºC for overnight and termed as enhanced hydrochar. The hydrochar yield was calculated by Eq. 1:

$$Y\ (\%) = (\text{amount of residue/amount of dried stock}) \times (\text{amount of enhanced residue/amount of hydrochar}) \times 100\% \quad (1)$$

Adsorption Experiment

A sequence of adsorption tests was performed to calculate the adsorption capacity of different adsorbent types. Important parameters affecting the adsorption process such as pH (ranging 2-10), adsorbent (hydrochar) contact time (up to 480 min), and temperature (25 to 65ºC) were observed in batch adsorption. For comparison, commercial activated carbon (CAC) was used as a control for adsorption performance.

In each adsorption test, the solutions were agitated in a closed water bath shaker at 150 rpm in contact with 0.1 g of adsorbent and 40 mL solution of Cr(VI) at designated temperature for a period of 8 hours in a sealed tube. The initial concentration of Cr(VI) solution was 100 mg/L. The diluted amount of (0.1 mol/L KOH or HCl) solution was prepared to adjust the pH of mixtures.

Adsorption isotherm batch tests were performed at various Cr(VI) concentrations (100 to 800 mg/L) for 8-hour intervals. The kinetics studies were also observed at 100 mg/L initial Cr(VI) concentration. Throughout this process, specimens were collected at different time intervals (ranging between 10 to 400 min). In addition, for thermodynamic studies, a separate series of tests were performed like kinetics experiments at 25ºC, 45ºC, and 65ºC.

An adsorption amount q_e (mg/g) and removal percentage (%) for Cr(VI) were calculated by Eqs 2 and 3, respectively:

$$\text{Removal Percentage (\%)} = \frac{(C_i - C_{eq})}{C_i} * 100\% \quad (2)$$

$$q_e = (C_i - C_{eq}) * V/M \quad (3)$$

…where C_i represents initial concentration, C_{eq} represents equilibrium of Cr(VI) in solution, M (mg) represents weight of the enhanced hydrochar, and V (mL) represents volume of solution.

Analytical Method

Cr(VI) ion concentrations in the effluent were analyzed by the UV-visible spectrophotometer using the 1,5-diphenylcarbazide method. The purple colored solution absorbance was analyzed at a wavelength of 540 nm after 10-15 min reaction time.

The BET surface area was determined by nitrogen adsorption in Quanta-chrome S1, USA at 77 K. The surface structure of untreated, treated and enhanced samples was studied after sputtering with a thin gold coating using a SEM (S-4800-HITACHI, Japan) at different magnifications. The (FTIR-Nicolet 67000, USA) equipment was employed to categorize the allocation of functional bands on all samples. The ranges were drawn from 400-4000 cm⁻¹ by applying the KBr pellet method. For cross check, SEM-EDS study was performed for observing the surface morphology of hydrochar, but there were no visible changes.

Detailed Discussion

Adsorption Capacity and Evaluation of Hydrochars on Cr(VI)

Two treatment methods of alkali and acid modification were employed to the hydrochar prepared from furfural residue, and their capacity was determined for Cr(VI) removal. Commercial activated carbon (CAC) was used as a control. The adsorption capacities of several adsorbents are described in Table 1, with some references to the earlier work.

The adsorption capacity of the furfural residue for Cr(VI) removal was 15.53 mg/g, which increased to 23.49 mg/g (i.e., 51.25%) after microwave-assisted hydrothermal treatment, suggesting that the hydrochar had better adsorption capacity than the raw biomass. The possible reason for this might be the fiber structure improved, and surface area stretched to more sites as a result of hydrothermal treatment [16]. Comparing the hydrothermal treatment of furfural residue with the alkali and acid modification, hydrochar capacity for Cr(VI) increased significantly after acid and alkali modification. However, alkali treatment had better adsorption capacity than the acid treatment. For example, the capacity of alkali enhanced hydrochar (0.05 N KOH) for Cr(VI) was 36.67 mg/g and acid enhanced hydrochar (0.05 N HCl) was 30.87 mg/g, which was 18.7% less than alkali treatment. An increase in the Cr(VI) adsorption with alkali modification (0.05 N KOH) could be due to the elimination of remaining organic material in the hydrochar by

Table 1. Adsorption capacity of Cr(VI) current study and published articles for comparison.

Material	Modification	Method	q_e (mg/g)	Removal (%)	Source
Furfural residue	Blank		15.53±0.37	38.82±1.31	This study
	Blank	MA-HTC	23.49±0.83	59.26±1.66	This study
	0.01 N KOH	MA-HTC	26.7±0.45	67.37±1.05	
	0.05 N KOH	MA-HTC	36.92±0.29	92.32±0.58	
	0.1 N KOH	MA-HTC	36.46±0.24	91.15±0.48	
	0.05 N HCl	MA-HTC	30.87±0.15	77.26±0.30	
	0.1 N HCl	MA-HTC	31.35±0.13	78.42±0.26	
Commercial activated carbon			30.76±0.11	76.77±0.22	This study
Peanut shells	Activation by KOH	HTC	16.26		[16]
Activated carbon	Oxidized with HNO_3	Commercial	13.3		[17]
Composite chitosan	Activation by fly ash	-	33.25		[18]
Tannin	By activated clay	-	24.09		[19]
P. vulgaris husk		Biosorbent	3.43		[8]
Eucalyptus sawdust	Activation by $ZnCl_2$	MA-HTC	7.63		[20]

MA-HTC: Microwave-assisted hydrothermal carbonization
HTC: Hydrothermal carbonization

potassium hydroxide treatment, and a decrease in the Cr(VI) adsorption with acid modification (0.05 N HCl) may be due to weak or destroyed structure. This shows that alkali treatment had an effective removal capacity for Cr(VI). Similarly, adsorption capacity of the alkali-enhanced hydrochar for Cr(VI) increased significantly than hydrothermal hydrochar, i.e., 23.49 mg/g to 36.67 mg/g, and the removal efficiency was improved to 91.72% from 59.29%.

An interesting factor here to discuss is that the commercial activated carbon showed lower removal efficiency than the alkali-treated hydrochar. For alkali enhanced hydrochar, the adsorption capacity was 36.67 (mg/g) with removal efficiency of 91.72%, and for activated carbon the adsorption capacity and removal efficiency were 30.75 (mg/g) and 76.77%, respectively, as shown in Table 1.

Optimum Conditions for Microwave-Assisted HTC and KOH Treatments

Microwave-assisted HTC temperature greatly affects the hydrochar yield and its properties. In the HTC process, the hydrochar surface holding oxygen-attached functional groups is influenced by the occurrence of the dehydration, decarboxylation, and hydrolysis reaction of lignocellulosic biomass. These appearances will have much influence on adsorption performance. Further increases in temperature, the thickness of the oxygen-containing functional groups and hydroxyl family of furfural residue from lignocellulosic biomass was decreased [21], which indicated that functional bands were reliant on applied temperature. Hence, the

selection of temperature was determined accordingly. The suggested temperatures for the microwave assisted hydrothermal carbonization were in the range of 180-250ºC [22].

As seen in Fig. 1a), the adsorption capacity was increased from 180ºC to 200ºC and it was decreased upon further increasing temperature from 200ºC to 220ºC. Conversely, the yield of the FR continuously decreased from 72.5% to 59.5% by increasing temperature from 180ºC to 220ºC. Zhang et al. studied the same trend of decreasing yield percentage for eucalyptus sawdust HTC to remove Cr(VI), where 47.61% of the yield was achieved [23]. Compared with microwave-assisted HTC, our study achieved 59.5% of the hydorchar yield. These results indicate that microwave-assisted HTC could produce higher hydrochar yield compared with the HTC method. Microwave-assisted HTC demonstrates that the hydrothermal reaction point developed more critically, which results in a decrease in oxygen content of lignocellulosic biomass due to water elimination [23, 24]. Therefore, it could be the cause of the decreased Cr(VI) adsorption performance. The balanced yield of solid residue and adsorption capacity suggested that 200ºC was the optimum temperature for microwave-assisted HTC for further experiments.

Alkali modification showed great effect in improving the adsorption capacity for Cr(VI) because of two main reasons. The first is to transform the exterior chemical features of hydrochar, for instance, active sites and external functional groups. The second reason is to expose choked pores to improve the porous structure of hydochar. For achieving suitable Cr(VI) adsorption capacity, different low-level potassium hydroxide

concentrations were examined to inspect the microwave-assisted HTC-prepared hydrochar at 200ºC. The graph representing hydochar yield and Cr(VI) adsorption capacity is shown in Fig. 1b).

We observed that (0.01 N KOH) modification did not show much impact on the adsorption capacity of Cr(VI), but as the concentration of KOH was increased from (0.01 N KOH to 0.05 N KOH), it greatly increased adsorption capacity from 26.70 to 36.92 mg/g. With the further increase in KOH concentration from (0.05 N KOH 0.1 N KOH), a slight decrease in the adsorption capacity of Cr(VI) was observed. Similarly, a slight decrease in the solid residue yield (i.e., from 78.32% to 71.28%) was also observed for 0.1 N KOH modifications. The reason could be the dissolved carbonaceous substance from microwave-assisted carbonization of raw biomass at medium-level alkali solution. These results showed that the low-level KOH treatment for furfural residue hydrochar was a beneficial technique to obtain highly efficient adsorbent. Considering better Cr(VI) capacity, high-yield hydrochar and operative cost, 0.05 N KOH treatment was taken as an optimal requirement.
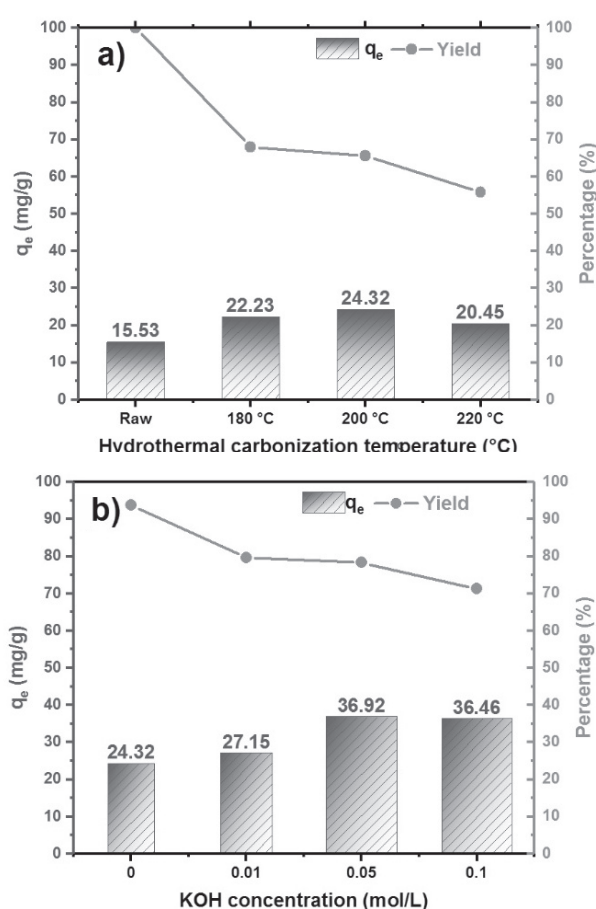
Experiments

pH and Contact Time Experiments

Fig. 2a) shows that the adsorption capacity of Cr(VI) was higher at lower pH. At pH 2, maximum adsorption capacity was observed, and at pH 4 there was a drastic decline in the Cr(VI) adsorption capacity. However, there was no radical change in Cr(VI) adsorption capacity between pH 4 to pH 10. The pH-dependent adsorption capacity should be due to the surface characteristics of the adsorbent and dissolved ions, which showed the extreme impact of pH. An electrostatic attraction is supported between the surface having charges and the Cr(VI) in the form of ($HCrO_4^-$); these pathways were created when the surface of carbon was covered by the huge number of H^+ in highly acidic form. The pH function is changed by Cr(VI) adsorption with CrO_4^{2-}, $HCrO_4^-$, H_2CrO_4, and $Cr_2O_4^{2-}$ ions acting as a principal family. At lower pH of 2, $HCrO_4^-$ was the dominant species [1, 6, 25]. Hence, adsorption capacity was noticed greater at lower pH. In contrast, hydroxide ions, which were plenty in the alkaline condition, would

Fig. 1. Effect of HTC temperature a) and KOH concentration b) on the adsorption capacity and hydrochar yield of Cr(VI).
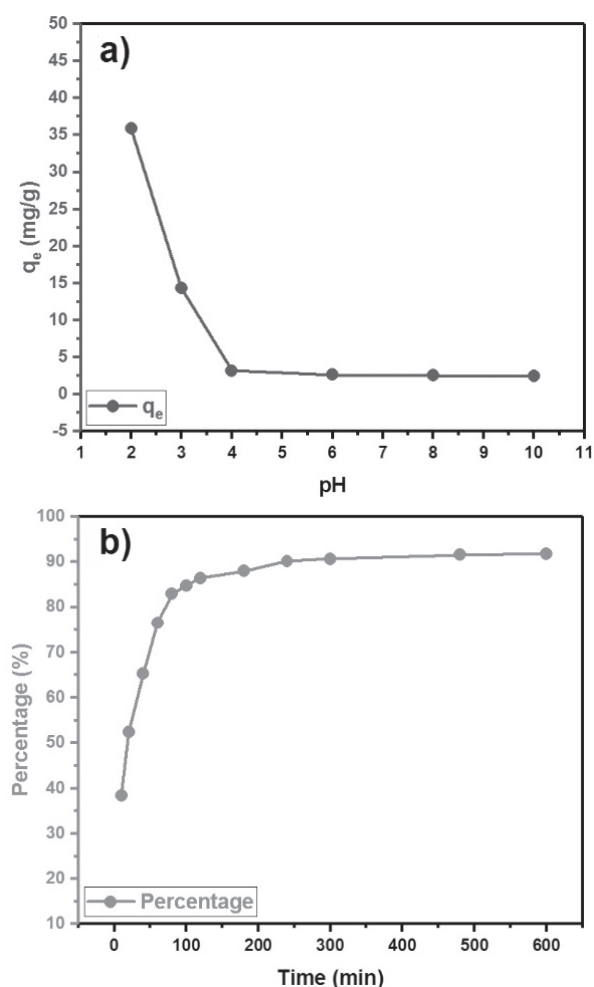

Fig. 2. Effect of different pH conditions a) and time interval b) on Cr(VI) adsorption capacity.

coat the entire surface area of hydrochar, thus resulting in the hydrochar carrying negative charges. At alkaline pH, CrO_4^{2-} was the dominant species with negative charge. Therefore, a repulsive force between adsorbate-adsorbent in the alkaline condition resulted in the lower adsorption capacity. A similar trend with higher Cr(VI) removal at pH 2 was observed from other researchers [24].

The contact time greatly influenced the adsorption capacity (see Fig. 2b). During the first 10 min, the removal percentage was 38.44%, and it became twice after 60 min. It could be said that the removal percentage improved with an increase in the time interval. However, the adsorption process reached equilibrium at 600 min. The same trend has been found by other researchers as well [23]. This shows that enhanced hydrochar requires less time to obtain equilibrium because it accumulates its space within pores. According to these results, the suggested time of adsorbent contact was 480 min – considered to be optimal time with 91.54% removal of Cr(VI).

Kinetics Studies

Usually, three sets of developments are associated in an adsorption method: (I) adsorption takes place on the interior surface where active sites of the porous adsorbent are present due to adsorbate molecules; (II) film diffusion, in which the drive of the adsorbate molecules goes toward the outer part of the adsorbent from the bulk amount of solution; (III) particle diffusion, which means the movement of adsorbate molecules inside adsorbent molecules [25].

As stated in Fig. 2b), a speedy adsorption process took place for the Cr(VI) removal just in 100 min, i.e., 84.4% at 298 K. Therefore, in order to compare the change in the adsorption process, two other temperatures of 318 K and 338 K were also analyzed as shown in Fig. 3 (a and b). By improving temperature from 298 K to 338 K, 86.71% Cr(VI) was removed in 60 min, and for temperature 338 K, 91.03% Cr(VI) was removed in 40 min. The experimental data of 298 K, 318 K, and 338 K was analyzed by pseudo first-order and pseudo second-order. The higher correlation coefficient (R^2) directed that the model effectively defined the kinetics of Cr(VI) adsorption [16].

Pseudo Frst-Order

Lagergren suggested a pseudo first-order kinetics model. The equation is stated as:

$$q_t = q_e(1 - e^{-k1t})$$

(4)

…where q_e (mg/g) represents quantity of Cr(VI) adsorbed per unit hydrochar/adsorbent mass at equilibrium state, q_t represents quantity of Cr(VI) per unit hydrochar/adsorbent mass at equilibrium state at

time interval t, and k_1 (min^{-1}) represents pseudo first-order rate constant. The pseudo first-order defines that at the solid/liquid interface adsorption degree is established on the solid performance. The curved lines were obtained by fitting an equation of pseudo first-order as shown in Fig. 3a) for 298 K, 318 K, and 338 K. The values of k_1 and q_e were derived from intercepts and slopes of the allotments. The correlation coefficient values acquired from pseudo first-order were less than the pseudo second-order. According to the experimental data, adsorption of Cr(VI) on the hydrochar did not fit for pseudo first-order, because pseudo first-order values for correlation coefficient were less than ($R<0.95$). Table 2 shows all the values for the correlation coefficient R^2.

Pseudo Second-Order

Adsorption kinetics could also be defined by a pseudo-second-order model. Its equation is written as [26];

$$\frac{t}{qt} = \frac{1}{k^2 q_e^2} + \frac{t}{qe}$$

(5)

…where k_2 (min^{-1}) represents pseudo second-order rate constant. The pseudo second-order describes the rate restraining as the chemical sorption exchanging number of electrons to link polar functional groups and adsorbent on an adsorbent from aqueous solution. The correlation coefficient R^2 of pseudo second-order was 0.98, 0.98 and 0.95 at 298 K, 318 K, and 338 K, respectively. This indicated that the pseudo second-order had higher results compared with the pseudo first-order as shown in Table 2.

Table 2. Fitting parameters for the Cr(VI) adsorption capacity on enhanced hydrochar.

Models	T (K)	298	318	338
Pseudo-first-order	k_1 (min^{-1})	0.0413	0.0548	0.0865
	q_e (mg/g)	35.35	38.47	39.49
	R^2	0.9462	0.9188	0.8885
Pseudo-second-order	k_2 (g/mg min)	0.00167	0.00214	0.00392
	q_e(mg/g)	38.31	41.22	41.34
	R^2	0.9884	0.9874	0.9527
Langmuir model	q_m (mg/g)	78.05	147.43	170.8
	k_1 (L/mg)	0.113	0.057	2.243
	R^2	0.7769	0.8128	0.8253
Freundlich model	k_f(mg$^{1-1/n}$L$^{1/n}$g^{-1})	27.66	48.64	80.72
	N	5.9288	5.3371	6.8858
	R^2	0.9724	0.9768	0.9393

Adsorption Isotherm

Langmuir and Freundlich are the most used sorption isotherm models for fitting data information. Langmuir supposes that the surface holds the same sorption sites and an uptake of sorbate molecule happens on the homogeneous surface by monolayer adsorption with no interface among the adsorption molecules. Freundlich works for dissimilar adsorption on heterogeneous surfaces.

In this model, heterogeneity is produced due to the existence of unlike functional groups on the adsorbent surface and numerous adsorbate-adsorbent interfaces [16].

Equations for both models are as follows:

$$\text{Langmuir:} \; q_e = \frac{q_m k_l C_{eq}}{1 + k_l C_{eq}} \tag{6}$$

$$\text{Freundlich:} \; q_e = k_f C_{eq} \frac{1}{n} \tag{7}$$

...where q_e represents mass of Cr(VI) adsorbed at equilibrium condition, C_{eq} represents equilibrium concentration, q_m represents maximal adsorption capacity, n termed as the relevant intensity constant, and k_l and k_f are the Langmuir and Freundlich constants, respectively.

Cr(VI) adsorption was calculated at various concentrations as presented in Fig. 3. The adsorption performance indicated an increase with increasing temperature and initial Cr(VI) concentration. For instance, Cr(VI) concentrations were increased from (100 to 800 mg/L), the adsorption capacity of Cr(VI) also indicated uptake from 34.80 mg/g to 78.08 mg/g at 298 K. The coefficient correlation R^2 of Freundlich model was all higher than the Langmuir model (see Table 2). This results in multi-layer adsorption on an external layer of required sites between Cr(VI) ions and external functional groups of the enhanced hydrochar. The Freundlich model constant (n), in the range 1 to 10, represents the promising adsorption practice [27]. This suggested that an effective contact occurred between Cr(VI) and hydrochar.
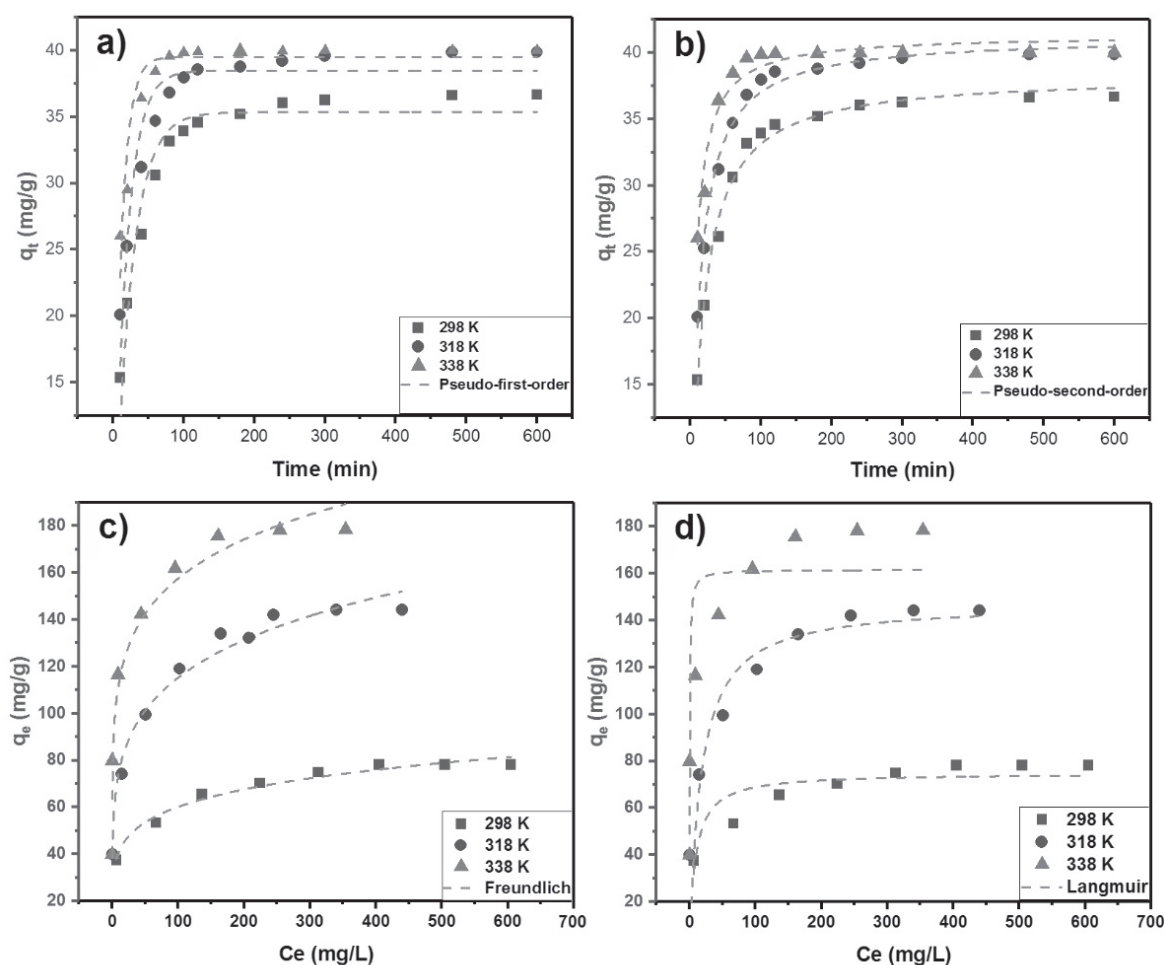

Fig. 3. Pseudo first-order a), pseudo second-order b), Freundlich model c) and Langmuir model d) for Cr(VI) adsorption at (298 K, 318 K and 338 K) temperatures.

Adsorption Thermodynamic Parameters

The adsorption thermodynamic process was adopted to examine the process involved in calculating Cr(VI) adsorption on hydrochar. The thermodynamic parameters ΔS^o, ΔH^o and ΔG^o were calculated by the following equations:

$$\Delta G^o = \Delta H^o - T\Delta S^o \qquad (8)$$

$$\Delta G^o = -RT\ln K^o \qquad (9)$$

$$K^o = \frac{aq_e}{C_e} \qquad (10)$$

$$\ln K^o = \frac{\Delta H^o}{RT} + \frac{\Delta S^o}{R} \qquad (11)$$

… where T represents absolute temperature, (a) represents hydrochar dosage (2.5 g/L), R represents

Table 3. BET surface area and pore distribution of the samples.

Material	BET Surface area (m^2/g)	Pore volume (cm^3/g)	Pore size (nm)
F_0	42.15	0.006488	2.455
F_1	46.98	0.008005	3.028
F_2	37.737	0.007205	3.084
F_3	26.93	0.006274	3.803

constant of universal gas (8.314 J $mol^{-1}K^{-1}$), and K^o represents sorption equilibrium constant defined by q_e/C_e, taken from adsorption isotherm (Freundlich or Langmuir model). Cr(VI) performance on the enhanced hydrochar is adequate for the Freundlich model. The values of ΔH^o, $\Delta G^{o,}$ and ΔS^o were derived by slope-intercept of $\ln K^o$ against $1/T$ as shown in Fig. 4a). The negative values of ΔH^o (-128.46 kJ mol^{-1}) directed an exothermic adsorption phenomenon, and the negative values of ΔS^o (-351.10 $JK^{-1}mol^{-1}$) specified the decrease in randomness at the solid and solution meeting point with some physical changes in the adsorbent-adsorbate at the time of adsorption method. This process was also examined in the adsorption of Acid Orange 52 by *Paulownia tomentosa* steud leaf powder [26]. Furthermore, the negative values of ΔG^o (-5.93 kJ mol^{-1} for 298 K, -15.35 kJ mol^{-1} for 318 K and -24.35 kJ mol^{-1} for 338 K) specified an actively promising adsorption process. The increase in ΔG^o by improving temperature indicated that the adsorption process was more encouraging at a higher temperature. This may conclude that higher temperature had shown frequent liaison between hydrochar and the Cr(VI) ions because several adsorption sites were damaged internally at the adsorbent bonding [28, 29].

The Arrhenius method was applied for calculating the adsorption activation energy by using the equation:

$$\ln k_2 = \ln A - \frac{E_a}{RT} \qquad (12)$$

...where R represents constant of universal gas (8.314 J/mol K), A represents pre-exponential factor, T represents absolute temperature, and k_2 (g/mg min) represents rate constant of pseudo second-order. Activation energy (E_a) was derived by slope-intercept of $\ln k_2$ against $1/T$ as shown in Fig. 4b). E_a for Cr(VI) on enhanced hydrochar was 18.51 $kJmol^{-1}$. The positive values of activation energy (E_a) represent the feasibility of the adsorption phenomenon. The lower value of E_a reflects that the rate-limiting stage in the chromium was controlled physically because physical adsorption often takes place at lower temperatures compared with the chemical adsorption. For chemical adsorption, the activation energy should be 40 kJ/mol.
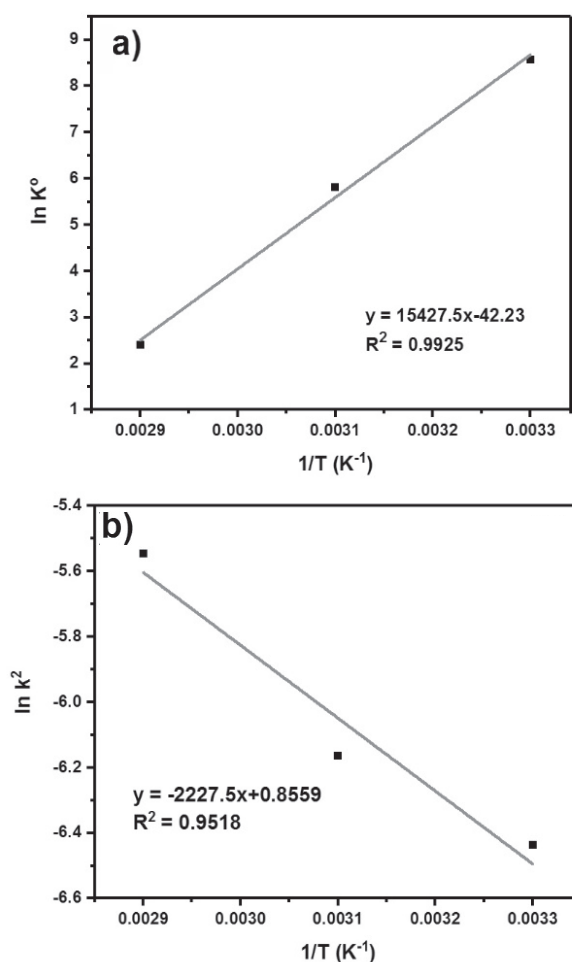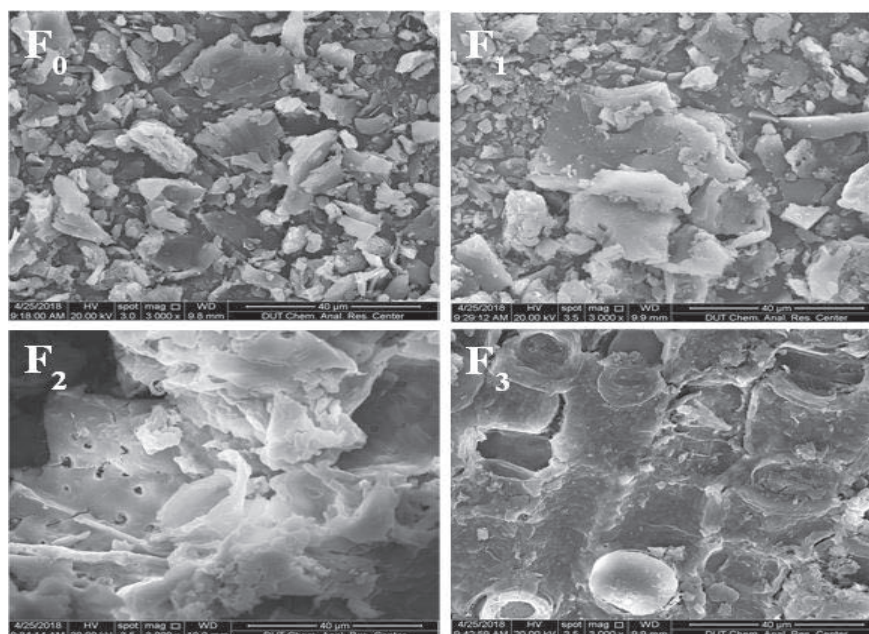

Fig. 4. Linear graph of ln K^o a) and ln k_2 b) against (1/T) for Cr(VI) adsorption on enhanced hydrochar at (298 K, 318 K, and 338 K) temperatures.

Fig. 5. SEM images of raw furfural residue (F_0), microwave-assisted hydrochar (F_1), alkali-modified (0.05 N KOH) hydrochar (F_2) and acid-modified (0.05 N HCl) hydrochar (F_3).

Characterization (BET and SEM)

BET specific surface area and BJH pore volume were analyzed as listed in Table 3. For raw material, the BET specific surface area was 42.15 m^{2}g^{-1}, which was lower than the microwave-assisted hydrochar. This showed that the BET specific area increased after pretreatment of the furfural residue (raw material). In contrast, the specific surface area and pore volume of enhanced hydrochar (alkali and acid treated) were lower than the microwave-assisted hydrochar. The pore size of the acid-treated hydrochar was higher than all other samples, but the pore volume was lower than all other samples. Similarly, the BET surface area of acid-treated hydrochar was also lower compared with others. This could be suggested from BET results that the pore size of treated (alkali and acid) hydrochar were higher than untreated and microwave-assisted hydrochar.

The surface structure of the raw material, microwave-assisted hydrochar and enhanced with low-level alkali and acid hydrochar are presented in Fig. 5. Furfural residues (untreated material) displayed a rigorous and irregular surface; this might be a reason for minimum adsorption capacity. After microwave-assisted HTC, the hydrochar were broken down into separate fibers as minor particles. The enhanced hydrochars were found to be more porous and smoother than that of untreated and HTC material. Conversely, the external structure of the alkali-treated hydrochar was more porous than acid-modified hydrochar. These results confirmed that alkali modification increased the porous structure and also improved the number of active sites on a fiber surface and consequently increased Cr(VI) performance.

Additional (SEM-EDS, QUANTA 450, Japan) study was performed for observing the surface morphology of hydrochar, but there were no visible changes observed. These results established the attachment of the chromium ions on the apparent part of the hydrochars at different temperatures after adsorption reaction.

FTIR Analysis

The surface functional groups were determined, and the spectra are illustrated in Fig. 6. The characteristic absorption peaks at 3414 cm^{-1} and 2992 cm^{-1} were allocated to the O-H and C-H stretching vibrations of the alkyl group, respectively [30]. The band at 1706 cm^{-1} was allocated in the range between 1735 cm^{-1} and 1045 cm^{-1} to the stretching vibration of the C=O bond of the acetyl group and C-O-C from hemicellulose [31]. The band at 1604 cm^{-1} was allocated in the range 1605 cm^{-1} and 1514 cm^{-1} for the benzene skeleton vibration, and the individual absorptions at 1513 cm^{-1} and 1317 cm^{-1} were related to the alkalyn ethers (-OH$_3$) and phenolic hydroxyl bending vibration, respectively. The band at 1056 cm^{-1} was attached with C-O stretching vibration. The lower intensity of the absorption peak at 902 cm^{-1} represents the damage of some β-glycoside bonds and the low intensity of bands at 1317 and 1164 cm^{-1}, verifying that hemicelluloses were set free from the cell wall of furfural residue. The functional groups were more abundant in produced samples than commercially activated carbons, as the results also directed that after alkali modification, the intensity of the carboxyl group improved. It could be assumed from the results that the surface structure of the enhanced hydrochar improved the Cr(VI) removal percentage.
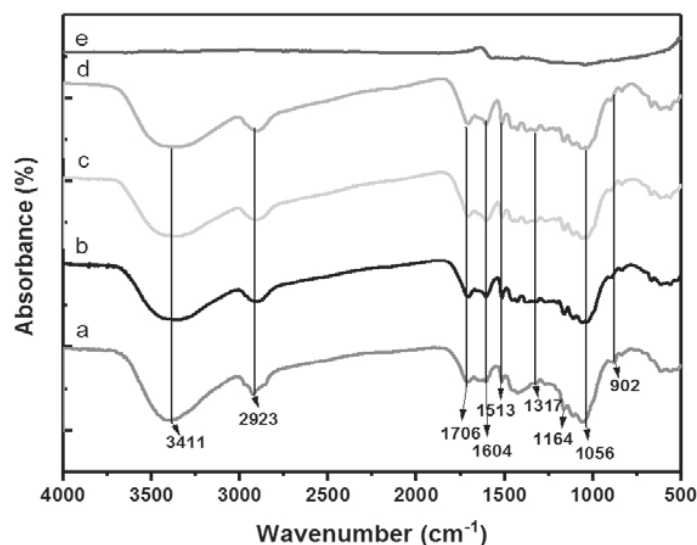
Fig. 6. Comparison of FTIR (furfural residue) a); hydrochar from microwave-assisted HTC at 200ºC b); alkali-enhanced (0.05 N KOH) hydrochar c); acid-enhanced hydrochar (0.05 N HCl) d); and commercially activated carbon (CAC) e).

Conclusions

This research clearly expresses that the combination of microwave-assisted HTC and modified furfural residue hydrochar with the low-level concentration of potassium hydroxide was highly efficient for Cr(VI) removal. The removal capacity was reliant on the initial solution concentration, agitation time, pH, and temperature. The microwave-assisted HTC temperature of 200ºC and low concentration of potassium hydroxide (0.05 N KOH) was found to be optimal, by which maximum adsorption capacity and removal percentage was achieved at 36.91 mg/g and 91.72%, respectively. The Freundlich model was the best fit for this study, which followed the pseudo second-order model. The negative value of ΔH^o represented an exothermic phenomenon of adsorption, the negative value of ΔS^o indicated decreasing randomness at the solid/solution interface, and the negative value of ΔG^o showed that the adsorption practice was more satisfied with the increasing temperature.

Acknowledgments

Conflict of Interest

There is no conflict of interest in this research.

References

1. PANDA H., TIADI N., MOHANTY M., MOHANTY C.R. Studies on adsorption behavior of an industrial waste for removal of chromium from aqueous solution. South African Journal of Chemical Engineering, **23**, 132, **2017**.
2. BAVARESCO J. Chromium Adsorption in Different Mineralogical Fractions, **27** (1), 106, **2017**.
3. ZHOU J., WANG Y., WANG J., QIAO W., LONG D., LING L. Journal of Colloid and Interface Science Effective removal of hexavalent chromium from aqueous solutions by adsorption on mesoporous carbon microspheres. Journal of Colloid And Interface Science, **462**, 200, **2016**.
4. LI L., LI Y., CAO L., YANG C. Enhanced chromium (VI) adsorption using nanosized chitosan fibers tailored by electrospinning. Carbohydrate Polymers, 125, 206, **2015**.
5. SAKULTHAEW C., CHOKEJAROENRAT C., POAPOLATHEP A. Hexavalent chromium adsorption from aqueous solution using carbon nano-onions (CNOs). Chemosphere, **184**, 1168, **2017**.
6. SUGASHINI S., BEGUM K.M.M.S. Preparation of activated carbon from carbonized rice husk by ozone activation for Cr(VI) removal. Xinxing Tan Cailiao/New Carbon Materials, **30** (3), 252, **2015**.
7. DING D., MA X., SHI W., LEI Z., ZHANG Z. Insights into mechanisms of hexavalent chromium removal from aqueous solution by using rice husk pretreated using hydrothermal carbonization technology. RSC Adv., **6** (78), 74675, **2016**.
8. SRIVASTAVA S., AGRAWAL S.B., MONDAL M.K. Characterization, isotherm and kinetic study of Phaseolus vulgaris husk as an innovative adsorbent for Cr(VI) removal. Korean Journal of Chemical Engineering, **33** (2), 567, **2016**.
9. NIZAMUDDIN S., BALOCH H.A., GRIFFIN G.J., MUBARAK N.M., BHUTTO A.W., ABRO R., ALI B.S. An overview of effect of process parameters on hydrothermal carbonization of biomass. Renewable and Sustainable Energy Reviews, **73** (December 2015), 1289, **2017**.

10. ZHANG J., AN Y., BORRION A., HE W., WANG N., CHEN Y., LI G. Process characteristics for microwave assisted hydrothermal carbonization of cellulose. Bioresource Technology, **259** (January), 91, **2018**.

11. ELAIGWU S.E., GREENWAY G.M. Microwave-assisted and conventional hydrothermal carbonization of lignocellulosic waste material: Comparison of the chemical and structural properties of the hydrochars. Journal of Analytical and Applied Pyrolysis, **118**, 1, **2016**.

12. VILELLA P.C., LIRA J.A., AZEVEDO D.C.S., BASTOS-NETO M., STEFANUTTI R. Preparation of biomass-based activated carbons and their evaluation for biogas upgrading purposes. Industrial Crops and Products, **109** (March), 134, **2017**.

13. REN G.J., WAN X.P. Adsorption of Alizarin Red from Aqueous Solution by Modified Furfural Residue. Advanced Materials Research, **826**, 163, **2013**.

14. BU L., TANG Y., GAO Y., JIAN H., JIANG J. Comparative characterization of milled wood lignin from furfural residues and corncob. Chemical Engineering Journal, **175** (1), 176, **2011v**

15. NIZAMUDDIN S., SIDDIQUI M.T.H., BALOCH H.A., MUBARAK N.M., GRIFFIN G., MADAPUSI S., TANKSALE A. Upgradation of chemical, fuel, thermal, and structural properties of rice husk through microwave-assisted hydrothermal carbonization. Environmental Science and Pollution Research, **25** (18), 17529, **2018**.

16. AL-OTHMAN Z.A., ALI R., NAUSHAD M. Hexavalent chromium removal from aqueous medium by activated carbon prepared from peanut shell: Adsorption kinetics, equilibrium and thermodynamic studies. Chemical Engineering Journal, **184**, 238, **2012**.

17. ZHAO N., WEI N., LI J., QIAO Z., CUI J., HE F. Surface properties of chemically modified activated carbons for adsorption rate of Cr(VI), **115**, 133, **2005**.

18. WEN Y., TANG Z., CHEN Y., GU Y. Adsorption of Cr(VI) from aqueous solutions using chitosan-coated fly ash composite as biosorbent. Chemical Engineering Journal, **175**, 110, **2011**.

19. LI W., TANG Y., ZENG Y., TONG Z., LIANG D., CUI W. Adsorption behavior of Cr(VI) ions on tannin-immobilized activated clay. Chemical Engineering Journal, **193-194**, 88, **2012**.

20. CHEN C., ZHAO P., LI Z., TONG Z. Adsorption behavior of chromium(VI) on activated carbon from eucalyptus sawdust prepared by microwave-assisted activation with $ZnCl_2$. Desalination and Water Treatment, **57** (27), 12572, **2016**.

21. KANG S., LI X., FAN J., CHANG J. Characterization of hydrochars produced by hydrothermal carbonization of lignin, cellulose, d-xylose, and wood meal. Industrial and Engineering Chemistry Research, **51** (26), 9023, **2012**.

22. BUNDHOO Z.M.A. Microwave-assisted conversion of biomass and waste materials to biofuels. Renewable and Sustainable Energy Reviews, **82** (September 2017), 1149, **2018**.

23. ZHANG X., ZHANG L., LI A. Eucalyptus sawdust derived biochar generated by combining the hydrothermal carbonization and low concentration KOH modification for hexavalent chromium removal. Journal of Environmental Management, **206**, 989, **2018**.

24. HU J., LO I.M.C., CHEN G. Comparative study of various magnetic nanoparticles for Cr(VI) removal. Separation and Purification Technology, **56** (3), 249, **2007**.

25. CHINGOMBE P., SAHA B., WAKEMAN R.J. Sorption of atrazine on conventional and surface modified activated carbons. Journal of Colloid and Interface Science, **302** (2), 408, **2006**.

26. AHMAD M.A., ALROZI R. Removal of malachite green dye from aqueous solution using rambutan peel-based activated carbon: Equilibrium, kinetic and thermodynamic studies. Chemical Engineering Journal, **171** (2), 510, **2011**.

27. KUMAR A.S.K., KALIDHASAN S., RAJESH V., RAJESH N. Application of cellulose-clay composite biosorbent toward the effective adsorption and removal of chromium from industrial wastewater. Industrial and Engineering Chemistry Research, **51** (1), 58, **2012**.

28. OGUZ E. Adsorption characteristics and the kinetics of the Cr(VI) on the Thuja oriantalis. Colloids and Surfaces A: Physicochemical and Engineering Aspects, **252** (2-3), 121, **2005**.

29. JAIN M., GARG V.K., KADIRVELU K., SILLANPÄÄ M. Adsorption of heavy metals from multi-metal aqueous solution by sunflower plant biomass-based carbons. International Journal of Environmental Science and Technology, **13** (2), 493, **2016**.

30. REN J., WANG W., YAN Y., DENG A., CHEN Q., ZHAO L. Microwave-assisted hydrothermal treatment of corncob using tin(IV) chloride as catalyst for furfural production. Cellulose, **23** (3), 1649, **2016**.

31. LI H., CHEN X., REN J., DENG H., PENG F., SUN R. Functional relationship of furfural yields and the hemicellulose-derived sugars in the hydrolysates from corncob by microwave-assisted hydrothermal pretreatment. Biotechnology for Biofuels, **8** (1), 1, **2015**.